

Sealed model and computation of hazardous waste landfill high voltage DC leakage detection^①

Yang Ping (杨萍)^②, Tian Jinwen, Wang Yanni, Xue Lin
(School of Information, Beijing Union University, Beijing 100101, P. R. China)

Abstract

According to the structural characteristics of hazardous waste landfill and the leakage current model of high voltage DC Landfill leakage detection, a sealed model is established and analyzed in detail. The detection layer of the hazardous waste landfill is considered as a sealed space and it is assumed that the source current flows through the leak entirely. The leak is regarded as a positive current resource $+I$ located at the current entrance or a negative resource $-I$ located at the current exit, which depends on the placement of the current supply. The electrical potential of an arbitrary in detection layer satisfies Poisson equation. The boundary condition is regarded as a natural boundary condition for the high resistivity of high density polyethylene (HDPE) membrane. Based on which a numerical calculation method is developed. Satisfactory agreement between experimental data and simulated data validates the analysis. Parametric studies show that a larger horizontal distance between the power supply electrode and leak and a smaller distance between the detector electrodes and the detected liner are helpful to leak location. More parametric curves show that parameters leaks can be detected effectively with optimum selection of field survey.

Key words: hazardous waste landfill, high voltage DC method, sealed space model

0 Introduction

High voltage DC potential detection has been developed to detect and locate leaks in geomembrane liner used in waste landfill to prevent environment from leachates contamination^[1,4]. To establish a basis for evaluating the technique, Parra developed a theoretical analysis method that characterized the three-dimensional response of single leaks^[5,6]. Wait developed a simple model and regarded the leak current as a point current source^[7,8]. Author's preliminary work showed that the leak current could be regarded as a negative current resource at the entrance or a positive one of the same size at the exit^[9]. Based on the fact that the single-liner landfills always had a large scale, a stratified medium model was established^[10-12], in which the waste material, the liner, and the soil under the liner were simulated as infinite in the horizontal direction. The relationship between the fraction of leak current I_0 to total current I , and the surface area of landfill has also been analyzed. And the results show that the relative amount of source current flowing through the leak

decreases as the size of the geomembrane liner increases. For a waste landfill having an area of 3600m^2 ($r_l = 60\text{m}$), 90 percent of the source current flows through the leak. Theoretically all the studies are about single-liner waste landfill. However hazardous waste landfills and storages usually use double geomembrane liners and the scale of which is only about several thousands of square meters. It is unreasonable to simulate the hazardous waste landfill as an infinite stratified model^[13], and the influence caused by side boundary is not negligible especially when a leak is near the boundary. Experiments in Chinese Research Academy of Environmental Sciences also demonstrate a big error when the stratified medium model is used to detect leaks in small scale double-liner landfill of 2000m^2 in area.

According to the structural characteristics of hazardous waste landfills and the leakage current model of high voltage leakage detection, a sealed model is deeply discussed. In this paper, the detection layer is considered as a sealed space and it is assumed that the source current flows through the leak entirely. The leak is regarded as a positive current resource $+I$ located at

① Supported by the National Basic Research Development Program of China (No. 2010CB428506), the National High Technology Research and Development Program (No. 2007AA061303) and Beijing Higher Education Young Elite Teacher Project (YETP1756).

② To whom correspondence should be addressed. E-mail: xxyangping@buu.edu.cn

Received on Oct. 14, 2014

the current entrance or a negative resource $-I$ located at the current exit, which depends on the placement of current supply. The electrical potential of an arbitrary in detection layer satisfies Poisson equation. The boundary condition is regarded as a natural boundary condition in view of the high resistivity of the HDPE membrane^[9,14]. On the basis of above assumptions, hazardous waste landfill leakage detection's sealed space model is established and analyzed in detail.

1 Principle

The electrical leak location method makes use of the high electrical resistivity of the geomembrane liner material. When no leak is presented, a voltage impressed across the liner produces a very low current flow. The low current density produces a relatively uni-

form potential distribution in the detection region. A leak in the geomembrane liner provides a conductive path for current flow, which produces an increase in the current density at the leak point. So the leak can be equaled to a current source. The localized current density causes an anomaly in the measured potential in the vicinity of the leak. Therefore, leaks can be located by measuring the potential distribution patterns in the material of the detection layer^[15]. The basic principle is shown in Fig. 1. For a double-lined hazardous waste landfill or storage, the detection layer can be regarded as a sealed space. Under this condition, the electrical potential distribution caused by a steady current is difficult to express analytically. So a new method is advanced to solve the problem of the potential distribution in the sealed detection region.

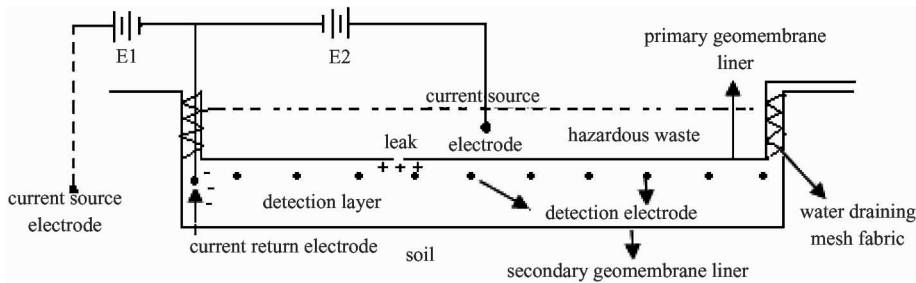


Fig. 1 Principle of hazardous waste landfill high voltage DC leakage detection

2 Model and analysis

2.1 Sealed space model

The detection layer can be taken as a sealed space encapsulated by high resistivity material. The upper surface and lower surface are primary geomembrane and secondary geomembrane respectively. They are all composed of HDPE membrane with resistivity $\rho_l = 10^{14} \Omega \cdot \text{m}$ ^[9]. The detection layer of depth h is full of clay soil with resistivity $\rho_c = 100 \Omega \cdot \text{m}$. A circular leak of radius a located at (x_0, y_0, z_0) is used to represent the leakage in geomembrane liner, which provides a channel for current flow. If the current source outside the sealed space is positive, then the current flows from the leak to the current return electrode located at (x_s, y_s, z_s) . Since it provides a high current density which is equivalent to a current resource, the leak in the high resistivity material is regarded as a positive current resource I_0 located at the center of the leak. So the electrical potential ϕ of an arbitrary point in detection layer is the superposition of electrical potential caused by the leakage current I_0 and the return electrode current $-I_s$. And the electrical potential ϕ satisfies Poisson equation

$$\nabla^2 \phi = f^{[16-18]}.$$

$$\text{Where } \nabla^2 = \frac{\partial^2}{\partial x^2} + \frac{\partial^2}{\partial y^2} + \frac{\partial^2}{\partial z^2},$$

$f = \rho_c I_0 \delta(x - x_0)(y - y_0)(z - z_0) - \rho_c I_s \delta(x - x_s)(y - y_s)(z - z_s)$, where ρ_c is the resistivity of the detection layer material, (x_0, y_0, z_0) and (x_s, y_s, z_s) are the coordinates of the leak and the current received electrode respectively. I_0 and I_s are the leakage current and the return electrode current. $\delta(x)$ is the δ function. The model is shown in Fig. 2.

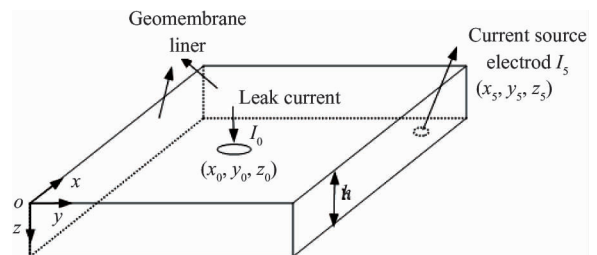


Fig. 2 Sealed space model of hazard waste landfill high voltage DC leakage detection

The interfaces continuity of potential and current density requires that^[16,17]:

$\frac{1}{\rho_c} \frac{\partial \phi}{\partial n} = \frac{1}{\rho_l} \frac{\partial \phi_l}{\partial n}$, where ρ_c and ρ_l are the resistivity of the detection layer material and gemembrane liner respectively.

For a highly resistive liner, $\rho_l \gg \rho_c$, which reduces the function to

$$\frac{\partial \phi}{\partial n} = \frac{\rho_c}{\rho_l} \frac{\partial \phi_l}{\partial n} \approx 0$$

where ϕ_l is the electrical potential distribution in the thin geomembrane liner. And n is outside normal direction. Considering the current density approximately equal to zero in n direction, it can be derived that $I_s = I_0$.

For a sealed region, it is difficult to give the analytical solution of the above Poisson equation. So a numerical calculation method is imported.

2.2 Mathematical analysis

2.2.1 Variational principle

The variational principle is known to us that, ^[18] a differential equation defined by

$$\mathcal{L}\phi = f \quad (1)$$

If \mathcal{L} is a selfadjoint operator, which means that $\langle \mathcal{L}\phi, \varphi \rangle = \langle \phi, \mathcal{L}\varphi \rangle$, then the function can be solved by obtaining the stagnation point of the function $F(\phi) = \frac{1}{2} \langle \mathcal{L}\phi, \phi \rangle - \frac{1}{2} \langle \phi, f \rangle - \frac{1}{2} \langle f, \phi \rangle$ (2)

where φ and ϕ are the arbitrary functions that have the same boundary conditions, $\langle \rangle$ is an operation defined as

$$\langle \phi, \varphi \rangle = \int_{\Omega} \phi \varphi^* d\Omega \quad (3)$$

where Ω expresses the region in question, $*$ represents the complex conjugate operation.

It is known to all that $\nabla^2 = \frac{\partial^2}{\partial x^2} + \frac{\partial^2}{\partial y^2} + \frac{\partial^2}{\partial z^2}$ is a selfadjoint operator under the circumstance of homogeneous boundary condition. So solving equation $\nabla^2 \phi = f$ at the boundary condition $\frac{\partial \phi}{\partial n} = 0$ is equivalent to solving the variational problem as follows:

$$\delta F(\phi) = 0 \quad (4)$$

$$\frac{\partial \phi}{\partial n} = 0 \quad (5)$$

where δ is variational operation, $F(\phi) = \frac{1}{2} \langle \nabla^2 \phi, \phi \rangle - \frac{1}{2} \langle \phi, f \rangle - \frac{1}{2} \langle f, \phi \rangle$ (6)

Because ϕ, f are real functions, $\langle \phi, f \rangle = \langle f, \phi \rangle$, and it is concluded that

$$F(\phi) = \frac{1}{2} \iiint_v [\nabla^2 \phi] \phi dv - \iiint_v \phi f dv \quad (7)$$

From the scalar Green theorem, it is deduced that ^[19]:

$$F(\phi) = \frac{1}{2} \iiint_v (\nabla \phi) \cdot (\nabla \phi) dv - \frac{1}{2} \oint_s \phi \frac{\partial \phi}{\partial n} ds - \iiint_v \phi f dv \quad (8)$$

where $\nabla = \frac{\partial}{\partial x} \hat{i} + \frac{\partial}{\partial y} \hat{j} + \frac{\partial}{\partial z} \hat{k}$, considering $\frac{\partial \phi}{\partial n} = 0$, then

$$F(\phi) = \frac{1}{2} \iiint_v [(\frac{\partial \phi}{\partial x})^2 + (\frac{\partial \phi}{\partial y})^2 + (\frac{\partial \phi}{\partial z})^2] dv - \iiint_v \phi f dv \quad (9)$$

2.2.2 Regional division

To express $F(\phi)$, the detection layer is divided into many small volume elements. Taking into account the tetrahedral element can partition the irregular boundary area, and the tetrahedral element is adopted in this paper. And the surface of the sealed region is divided into many small triangular elements. M is used to express the total amount of the tetrahedral elements, $i = 1, 2, 3, 4$ expresses the endpoint of the tetrahedral element, the size of $4 \times M$ array $n(i, e)$ connects the element and the endpoint, where $e \in [1, M]$, for example, $n(3, 5)$ means the third endpoint of the fifth element. Moreover, the stagnation point of $F(\phi)$ can be solved with no need for considering the boundary condition $\frac{\partial \phi}{\partial n} = 0$ for it will be satisfied automatically.

2.2.3 Interpolation

After regional discrete, unknown function ϕ in every tetrahedral element need to be expressed. Hence the tetrahedral element as Fig. 3 is taken into account. In every tetrahedral element e , the unknown function ϕ can be described as ^[20-22]

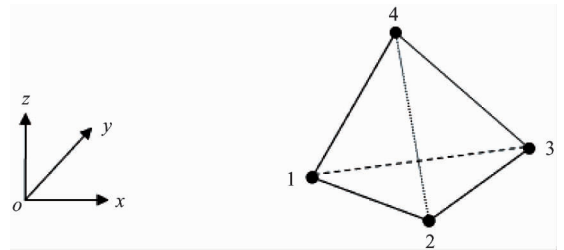


Fig. 3 Linear tetrahedron cell

$$\phi^e(x, y, z) = a^e + b^e x + c^e y + d^e z \quad (10)$$

Impose $\phi^e(x, y, z) = a^e + b^e x + c^e y + d^e z$ to the four endpoints, and ϕ at endpoint j of e element is expressed as ϕ_j^e , the follow functions will be got:

$$\phi_1^e = a^e + b^e x_1^e + c^e y_1^e + d^e z_1^e \quad (10-1)$$

$$\phi_2^e = a^e + b^e x_2^e + c^e y_2^e + d^e z_2^e \quad (10-2)$$

$$\phi_3^e = a^e + b^e x_3^e + c^e y_3^e + d^e z_3^e \quad (10-3)$$

$$\phi_4^e = a^e + b^e x_4^e + c^e y_4^e + d^e z_4^e \quad (10-4)$$

Based on the above equations, it can be deduced that:

$$a^e = \frac{1}{6V^e} \begin{vmatrix} \phi_1^e & \phi_2^e & \phi_3^e & \phi_4^e \\ x_1^e & x_2^e & x_3^e & x_4^e \\ y_1^e & y_2^e & y_3^e & y_4^e \\ z_1^e & z_2^e & z_3^e & z_4^e \end{vmatrix} = \frac{1}{6V^e} (a_1^e \phi_1^e + a_2^e \phi_2^e + a_3^e \phi_3^e + a_4^e \phi_4^e) \quad (11-1)$$

$$b^e = \frac{1}{6V^e} \begin{vmatrix} 1 & 1 & 1 & 1 \\ \phi_1^e & \phi_2^e & \phi_3^e & \phi_4^e \\ y_1^e & y_2^e & y_3^e & y_4^e \\ z_1^e & z_2^e & z_3^e & z_4^e \end{vmatrix} = \frac{1}{6V^e} (b_1^e \phi_1^e + b_2^e \phi_2^e + b_3^e \phi_3^e + b_4^e \phi_4^e) \quad (11-2)$$

$$c^e = \frac{1}{6V^e} \begin{vmatrix} 1 & 1 & 1 & 1 \\ x_1^e & x_2^e & x_3^e & x_4^e \\ \phi_1^e & \phi_2^e & \phi_3^e & \phi_4^e \\ z_1^e & z_2^e & z_3^e & z_4^e \end{vmatrix} = \frac{1}{6V^e} (c_1^e \phi_1^e + c_2^e \phi_2^e + c_3^e \phi_3^e + c_4^e \phi_4^e) \quad (11-3)$$

$$d^e = \frac{1}{6V^e} \begin{vmatrix} 1 & 1 & 1 & 1 \\ x_1^e & x_2^e & x_3^e & x_4^e \\ y_1^e & y_2^e & y_3^e & y_4^e \\ \phi_1^e & \phi_2^e & \phi_3^e & \phi_4^e \end{vmatrix} = \frac{1}{6V^e} (d_1^e \phi_1^e + d_2^e \phi_2^e + d_3^e \phi_3^e + d_4^e \phi_4^e) \quad (11-4)$$

where

$$V^e = \frac{1}{6} \begin{vmatrix} 1 & 1 & 1 & 1 \\ x_1^e & x_2^e & x_3^e & x_4^e \\ y_1^e & y_2^e & y_3^e & y_4^e \\ z_1^e & z_2^e & z_3^e & z_4^e \end{vmatrix} \text{ is regarded as the tetrahedral element's volume.}$$

Coefficient a_j^e, b_j^e, c_j^e and d_j^e can be derived by expanding the determinant.

Taking the Coefficient a^e, b^e, c^e, d^e back to $\phi^e(x, y, z) = a^e + b^e x + c^e y + d^e z$, the following is got:

$$\phi^e(x, y, z) = \sum_{j=1}^4 N_j^e(x, y, z) \phi_j^e \quad (12)$$

where $N_j^e(x, y, z) = \frac{1}{6V^e} (a_j^e + b_j^e x + c_j^e y + d_j^e z)$ has the property^[21]:

$$N_i^e(x_j, y_j, z_j) = \delta_{ij} = \begin{cases} 1 & i = j \\ 0 & i \neq j \end{cases} \quad (13)$$

2.2.4 Calculation formula of Ritz method

After regional discretion and interpolation,

Eq. (9) can be expressed as

$$F(\phi) = \sum_{e=1}^M F^e(\phi^e) \quad (14)$$

where M is the total amount of the tetrahedral element,

$$F^e(\phi^e) = \frac{1}{2} \iiint_{v^e} [(\frac{\partial \phi^e}{\partial x})^2 + (\frac{\partial \phi^e}{\partial y})^2 + (\frac{\partial \phi^e}{\partial z})^2] dv - \iiint_{v^e} \phi^e f dv \quad (15)$$

v^e is the volume of e unit, combine $\phi^e(x, y, z) = \sum_{j=1}^4 N_j^e(x, y, z) \phi_j^e$ and $F^e(\phi^e)$ given above. Follow formula can be deduced

$$\frac{\partial F^e}{\partial \phi_i^e} = \sum_{j=1}^4 \phi_j^e \iiint_{v^e} [\frac{\partial N_i^e}{\partial x} \frac{\partial N_j^e}{\partial x} + \frac{\partial N_i^e}{\partial y} \frac{\partial N_j^e}{\partial y} + \frac{\partial N_i^e}{\partial z} \frac{\partial N_j^e}{\partial z}] dv - \iiint_{v^e} N_i^e f dv \quad (16)$$

The matrix form is

$$\left\{ \frac{\partial F^e}{\partial \phi^e} \right\} = [K^e] \{ \phi^e \} - \{ b^e \} \quad (17)$$

where:

$$K_{ij}^e = \iiint_{v^e} [\frac{\partial N_i^e}{\partial x} \frac{\partial N_j^e}{\partial x} + \frac{\partial N_i^e}{\partial y} \frac{\partial N_j^e}{\partial y} + \frac{\partial N_i^e}{\partial z} \frac{\partial N_j^e}{\partial z}] dv \quad (18)$$

$$b_i^e = \iiint_{v^e} N_i^e f dv \quad (19)$$

Based on the fundamental formulae^[17,18]:

$$\iiint_{v^e} (N_1^e)^k (N_2^e)^l (N_3^e)^m (N_4^e)^n dv = \frac{k!l!m!n!}{(k+l+m+n+3)!} 6V^e, K_{ij}^e \text{ and } b_i^e \text{ are simplified as}$$

$$K_{ij}^e = \frac{1}{36V^e} (b_i^e b_j^e + c_i^e c_j^e + d_i^e d_j^e) \quad (20)$$

$$b_i^e = \frac{V^e}{4} f^e \quad (21)$$

2.2.5 Combined into equations

Based on Eq. (17), combining with all units, and imposing the Stagnation point condition to F , the following equation is got:

$$\left\{ \frac{\partial F}{\partial \phi} \right\} = \sum_{e=1}^M \left\{ \frac{\partial F^e}{\partial \phi^e} \right\} = \sum_{e=1}^M ([\overline{K^e}] \{ \overline{\phi^e} \} - \{ \overline{b^e} \}) = 0 \quad (22)$$

The compact form is

$$[K] \{ \phi \} = \{ b \} \quad (23)$$

where

$$[K] = \sum_{e=1}^M [\overline{K^e}] \text{ and } \{ b \} = \sum_{e=1}^M \{ \overline{b^e} \}$$

2.2.6 Solution of the equations

Generally, K in Eq. (22) is divided into an Upper triangular matrix U and a lower triangular matrix L . That is

$$K = LU$$

Firstly, the matrix equation is solved: $L\varphi = b$ (24)

Then: $U\varphi = \varphi$ (25)

Use the Crout decomposition method^[19-21]

$$u_{ii} = 1 \quad i = 1, 2, 3, \dots, n \quad (26)$$

$$l_{ij} = k_{ij} - \sum_{k=1}^{j-1} l_{ik}u_{kj} \quad i \geq j \quad (27)$$

$$u_{ij} = \frac{1}{l_{ii}}(k_{ij} - \sum_{k=1}^{i-1} l_{ik}u_{kj}) \quad i < j \quad (28)$$

Through step forward, φ ^[22] is obtained

$$\varphi_1 = \frac{b_1}{l_{11}} \quad (29)$$

$$\varphi_i = \frac{1}{l_{ii}}(b_i - \sum_{k=1}^{i-1} l_{ik}\varphi_k) \quad i > 1 \quad (30)$$

Then, through step backward, the value of ϕ at the endpoint of a tetrahedral element is got.

$$\phi_n = \varphi_n \quad (31)$$

$$\phi_i = \varphi_i - \sum_{k=i+1}^n u_{ik}\phi_k \quad i < n \quad (32)$$

Finally, the value of ϕ at any point (x, y, z) can be obtained by element interpolating function.

3 Experiment and computation

3.1 Experiment verification

To verify the validity of the model in locating leaks in geomembrane liner of hazard waste landfill, experiments are made at a double-lined simulated land-

fill (10m × 10m × 0.4m). As is shown in Fig. 1, the landfill has two HDPE geomembrane liners with the thickness $t = 2\text{mm}$. The primary liner is covered with water of 0.3m in depth. The detection layer of 0.4m depth is between the primary liner and the secondary liner. Fixed detection electrodes are buried in the detection layer during the construction of the simulated landfill, with 1m-distance from each other and 0.1m from the primary liner. One leak is on the primary liner, the other leak is on the secondary liner. Two leaks are on the center of the 11 × 11 measurement electrodes. To create an electrical flow through the leak, the positive electrode of DC current source is placed in the water used to simulate the hazardous waste when detecting primary liner or in soil when detecting secondary liner, the negative electrode (current return electrode) of DC current source is placed in the detection layer at the position (9.9, 0.1, 0.08) to form the current passage. The fixed electrode measurement is carried out by installing a potential reference electrode at the position (10, 5, 0.08), which is used to provide a common reference point for the potential measurements (the coordinate system in Fig. 2 is referenced here). 121 data are collected over an area of 100m².

Table 1 shows the sealed model parameters for locating leaks. These parameters come from the test result of the facility.

Table 1 Model parameters^[23,24]

parameter	value	parameter	value
Detection electrode spacing $s(\text{m})$	1	Survey depth $d(\text{cm})$	10
Clayer resistivity $\rho_c (\Omega \cdot \text{m})$	48	Current magnitude $I(\text{mA})$	80
Size of tetrahedron cell's side length (cm)	5	The structure (L × W × H) of the sealed space(m)	10 × 10 × 0.4

Table 2 shows the experimental data collected from the detection electrodes laid on two crossed lines under or above the leaks and the corresponding simulated value based on sealed model. Leak 1 is located at the center of the primary liner. Leak 2 is located at the center of the secondary liner. The relative errors are also shown in Table 2.

Data in Table 2 show that the relative errors between simulated data and experimental data are less than 5%. Considering the location error of detection electrodes during construction, the errors in measurement and the influence caused by noise and other factors, it can be concluded that the analysis method given above is valid.

3.2 Parameter study

The parameter studies below are aimed at charactering the performance of the method for variations in the detection layer material electrical parameters, the contamination, the detection electrodes and current supply electrode position, and the detection layer depth. The result demonstrates the general applicability of the method and may be used to optimize the technique for specific landfill survey application.

3.2.1 Effect of detection layer resistivity

The detection layer material's resistivity ρ_c is controllable, which can be changed during the construction of a waste landfill. Fig.4 shows the anomaly responses for varying detection layer resistivity for detec-

tion electrodes survey data measured at a depth of $d = 0.05\text{m}$ below the primary liner. These results demonstrate that the strength of the anomaly response is in-

creased and leak detectability is improved for high detection layer resistivity.

Table 2 Comparison of experimental data and simulated data of two survey lines (V)

leak 1						leak 2					
The east-west detection line			The south-north detection line			The east-west detection line			The south-north detection line		
Simulat- ed data	Experimen- tal data	Relative errors	Simulat- ed data	Experimen- tal data	Relative errors	Simulat- ed data	Experimen- tal data	Relative errors	Simulat- ed data	Experimen- tal data	Relative errors
0	0	0.00%	0.001	0.001	0.00%	0	0	0.0002	0	0	
0.185	0.177	4.52%	0.186	0.193	3.63%	0.185	0.189	2.12%	0.186	0.19	2.11%
0.732	0.741	1.21%	0.733	0.717	2.23%	0.732	0.756	3.17%	0.733	0.758	3.30%
1.647	1.586	3.85%	1.648	1.692	2.60%	1.647	1.678	1.85%	1.684	1.624	3.69%
3.123	3.221	3.04%	3.123	3.134	0.35%	3.121	3.14	0.61%	3.123	3.068	1.79%
16.061	16.081	0.12%	16.061	16.216	0.96%	5.972	5.895	1.31%	5.972	5.764	3.61%
3.947	3.868	2.04%	3.947	3.988	1.03%	3.947	4.058	2.74%	3.946	4.037	2.25%
3.236	3.321	2.56%	3.236	3.135	3.22%	3.238	3.174	2.02%	3.237	3.323	2.59%
2.957	2.889	2.35%	2.957	2.979	0.74%	2.958	3.029	2.34%	2.957	3.018	2.02%
2.838	2.792	1.65%	2.838	2.914	2.61%	2.839	2.859	0.70%	2.839	2.794	1.61%
2.805	2.767	1.37%	2.805	2.736	2.52%	2.805	2.804	0.04%	2.805	2.818	0.46%

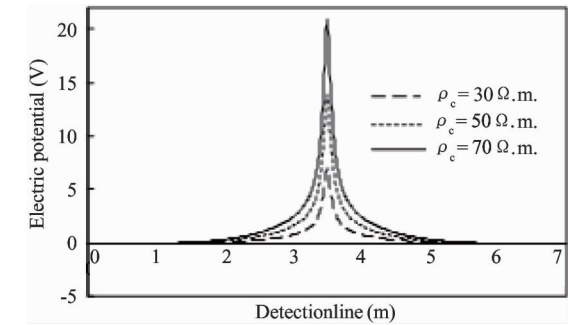


Fig. 4 Distribution of the electric potential besides the leak for different resistivity of the detecting liner

3.2.2 Effect of the inhomogeneity of detection layer medium

Leak in the liner allows the leachates from the waste materials to detection layer, so the resistivity of contaminated region will decrease. ρ_c' is used here to present the resistivity of contaminated region. Fig.5 shows the family of leak anomaly responses for different contaminated hemisphere r and $\rho_c' = 10\Omega.m$. The anomaly decays rapidly as the contaminated radius increases, so the leakage should always be conducted timely.

3.2.3 Effect of detection electrodes depth

A family of leak anomaly responses for several detection electrodes depths below a single leak located in the primary liner is shown in Fig.6, which indicates

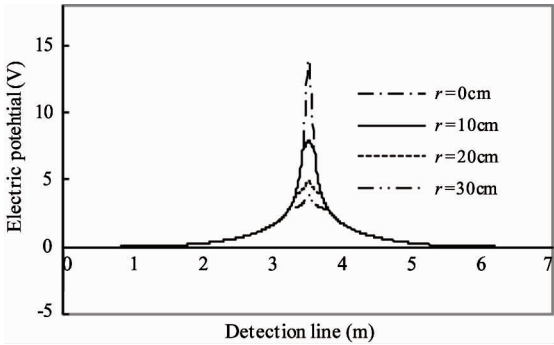


Fig. 5 Distribution of the electric potential besides the leak for different radius of the pollution area

the substantial improvement gained in detection sensitivity when the detection electrodes are closer to the detection liner. That is to say, the survey should always be conducted to the detection liner as close as possible.

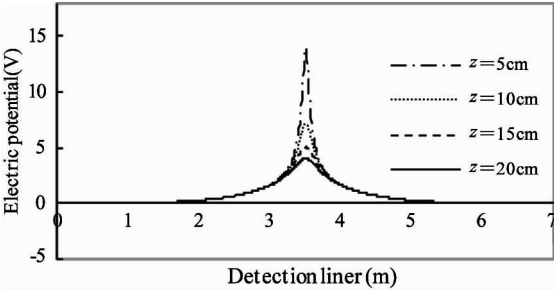


Fig. 6 Distribution of the electric potential besides the leak for different vertical distance from the leak

3.2.4 Effect of leak current

Fig.7 shows the anomaly responses for different leak current. The results illustrate that the higher the leak current, the higher the detectability.

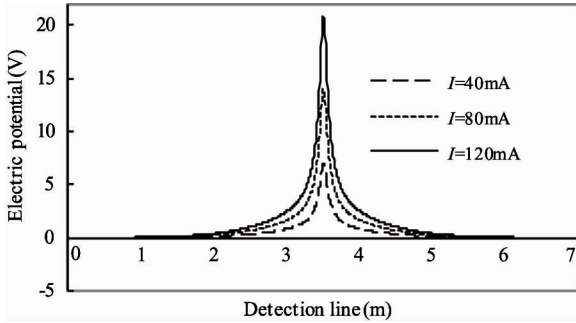


Fig. 7 Distribution of the electric potential besides the leak for different current of the leak

3.2.5 Effect of the offset distance from the leak to current resource electrode

The offset distance of the leak to current resource electrode affects the anomaly response. To illustrate this characteristic, Fig.8 presents the distribution of the electric potential besides the leak for different horizontal distance horizontal distance (hd) from leak to source electrode. In Fig. 9, the distribution for different vertical distance vertical distance (vd) from leak to

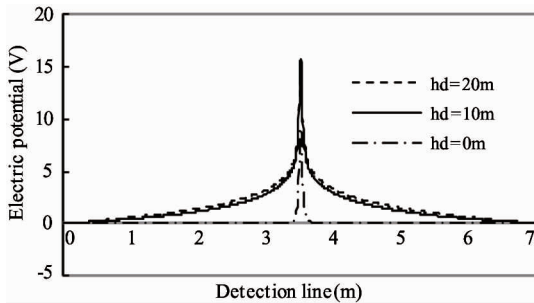


Fig. 8 Distribution of the electric potential besides the leak for different horizontal distance (hd) from leak to source electrode

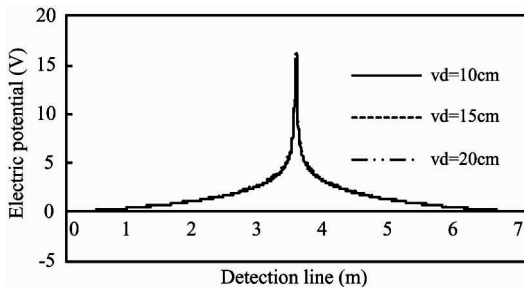


Fig. 9 Distribution of the electric potential besides the leak for different vertical distance (vd) from leak to source electrode

source electrode is given. As expected, when the horizontal distance is far enough ($> 10\text{m}$), the vertical distance from leak to source electrode has little influence on the leak anomaly responses. But when the source electrode is just below a leak, the range of the leak anomaly responses is very small. It is hard to detect the leak under this circumstance. Hence, in order to detect the entire region of a landfill, there are at least two power supply electrodes in the detection layer.

4 Conclusion

For a hazardous waste landfill, when a high DC voltage is imposed on the both sides of the geomembrance liner, the detection liner can be seen as a sealed space excited by leakage current and the return electrode current. The leakage current is a positive current resource $+I$ located at the current entrance or a negative resource $-I$ located at the current exit. The electrical potential of an arbitrary in detection layer satisfies the Poisson equation. The boundary conditions satisfy natural boundary condition. Parametric studies show that big magnitude of leak current, high resistivity of detection liner, large horizontal distance between the power supply electrode and leak and small distance between the detector electrodes and the detected liner are helpful to leak location, but the vertical distance from leak to source electrode has little influence on the leak anomaly responses when the horizontal distance is far enough ($> 10\text{m}$).

The numerical method is effective in solving the problem of potential distribution in even an irregular region. But there exists some shortage such as low computational efficiency. How to improve the computation efficiency will be the emphasis for further research.

Reference

- [1] Darilek G T, Laine D L, Parra J O. The electrical leak location method for geomembrane liners - Development and application. In: Proceedings of the Industrial Fabrics Association International Geosynthetics, San Diego, USA, 1989. 21-23
- [2] Darilek G T, Laine D L. Understanding electrical leak location systems of geomembrane liners and avoiding specifications pitfalls. In: Proceedings of the 10th National Conference, Superfund, Washington, D C, USA, 1989. 27-29
- [3] Smith B, Darilek G, Laine D. Enhanced geomembrane CQA through proper application of geomembrane leak location surveys. In: Proceedings of the Geosynthetics 2007 Conference Proceedings, Washington D C, USA, 2007. 16-19
- [4] Darilek G, Laine D. Experience with geosynthetic clay

- liners as a conductive layer in geomembrane leak location surveys. *Geosynthetics*, 2007, 14 (6):30-33
- [5] Parra J O. Electrical response of a leak in a geomembrane liner. *Geophysics*, 1988, 53 (11):1445-1452
- [6] Parra J O, Owen T E. Model studies of electrical leak detection in geomembrane lined impoundments. *Geophysics*, 1988, 53(11):1453-1458
- [7] Wait J R. Complex resistivity of the Earth. *Progress in Electromagnetic Research*, 1989, 1(1):171-175
- [8] Wait J R. Simple model for current leakage in insulating liner. *IEEE transactions on geoscience and remote sensing*, 1994, 32(2):472-474
- [9] Yang P, Nai C X, Dong L. Leak current model in leakage detection of HDPE liner using high voltage DC method. *Acta Scientiae Circumstantiae*, 2005, 25 (10):1261-1364 (in Chinese)
- [10] Yang P, Dong L, Wang Q. Multimedia model of single-liner landfill high voltage DC leak detection. *China Environmental Science*, 2008, 28(1):63-67
- [11] Zhao X C, Yang P, Zhang Y D, et al. Finite element simulation of high voltage direct current electricity technology for double liner landfill leakage detection. *China Environmental Science*, 2007, 27(1):76-79
- [12] Guan S P, Nai C X, Dong L, et al. A direct current resistance circuit model for landfill leak detection. *Acta Scientiae Circumstantiae*, 2010, 30(6):1188-1192
- [13] Wang Z C, Chen Y Y. Hazardous waste landfill leakage detection based on transmission lines model. *Advances in Information Sciences and Service Sciences*, 2011, 3(9):17-24
- [14] Nai C X, Dong L, Wang Q, et al. The stratified medium model for leakage detection in double liner landfills. *Research of Environmental Sciences*, 2008, 21(6):30-34
- [15] Yang P, Jiang Y X, Wang Y N, et al. Study on double-liner landfill leak location algorithm. *Journal of Beijing Union University*, 2013, 27(1):81-85
- [16] Guan S P, Wang Y L, Nai C X. Application of electrical leak detection method in double-lined landfills. *China Environmental Science*, 2011, 31(12):2013-2017
- [17] Qiao S, Zhou M Y, Bai L. Theory of Exploration Electromagnetic Field. Beijing: China University Mining Technology Press, 1989. (In Chinese)
- [18] Yao D Z, Liang J B. Method of Mathematics and Physical. Wuhan: Wuhan University Press, 1997. (In Chinese)
- [19] Lang K M. Method of Mathematics and Physical. Beijing: High Education Press, 1997. (In Chinese)
- [20] Zong Z H, Gao M L, Xia Z H. Finite element model validation of the continuous rigid frame bridge based on structural health monitoring part I; FE model updating based on the response surface method. *China Civil Engineering Journal*, 2011, 2(44):90-98
- [21] Merla A, Donato D, Fazio D. Differential thermal infrared imaging for environmental inspection. *Journal of applied remote sensing*, 2014, 8(11):117-123
- [22] Abuel N, Hossam M. Bouazza A. Numerical characterization of advective gas flow through GM/GCL composite liners having a circular defect in the geomembrane. *Journal of Geotechnical and Geoenvironmental Engineering*, 2009, 135(11):1661-1671
- [23] Gao M L. Study on the Finite Element Model Validation of the Continuous Rigid Frame Bridge Based on Structural Health Monitoring:[Ph. D dissertation]. Fuzhou: Fuzhou University, 2008
- [24] Chen Y Y, Nai C X, Dong L, et al. Landfill leakage detection based on boundary localization method. *Research of Environmental Sciences*, 2012, 25(3):346-351

Yang Ping, born in 1974. She received her Ph. D and M. S degrees from college of Mechatronic Engineering of China Mining & Technology University (Beijing) in 2006 and 2003 respectively. She also received her B. S degrees from XinYang Normal University in 1997. Her research interests include signal acquisition & processing and mathematical modeling.